

# Surface features of polymer electrolyte membranes for fuel cell applications: An approach using S2p XPS analysis

Lam Hoang Hao<sup>1,2</sup>, Dinh Tran Trong Hieu<sup>1,2,3</sup>, Tran Thanh Danh<sup>1,2</sup>, Tran Hoang Long<sup>1,2</sup>, Huynh Truc Phuong<sup>2,4</sup>, Le Quang Luan<sup>5</sup>, Tran Van Man<sup>2,6</sup>, Luu Anh Tuyen<sup>7</sup>, Pham Kim Ngoc<sup>1,2</sup>, Tran Duy Tap<sup>1,2,\*</sup>



Use your smartphone to scan this QR code and download this article

<sup>1</sup>Faculty of Materials Science and Technology, University of Science, 227 Nguyen Van Cu, District 5, Ho Chi Minh 700000, Viet Nam

<sup>2</sup>Viet Nam National University, Ho Chi Minh City, Viet Nam

<sup>3</sup>Physics Laboratory, Le Thanh Ton high school, 124, 17 street, District 7, Ho Chi Minh 700000, Viet Nam

<sup>4</sup>Faculty of Physics and Engineering Physics, University of Science, 227 Nguyen Van Cu, District 5, Ho Chi Minh 700000, Viet Nam

<sup>5</sup>Biotechnology Center of Ho Chi Minh City, 2374 Highway 1, District 12, Ho Chi Minh 700000, Viet Nam

<sup>6</sup>Applied Physical Chemistry Laboratory, Department of Physical Chemistry, University of Science, 227 Nguyen Van Cu, District 5, Ho Chi Minh 700000, Viet Nam

<sup>7</sup>Center for Nuclear Techniques, Viet Nam Atomic Energy Institute, 217 Nguyen Trai, District 1, Ho Chi Minh 700000, Viet Nam

## Correspondence

**Tran Duy Tap**, Faculty of Materials Science and Technology, University of Science, 227 Nguyen Van Cu, District 5, Ho Chi Minh 700000, Viet Nam  
Viet Nam National University, Ho Chi Minh City, Viet Nam  
Email: tdtap@hcmus.edu.vn

## History

- Received: 2021-05-08
- Accepted: 2021-08-31
- Published: 2021-09-07

DOI : 10.32508/stdj.v24i3.2556



## Copyright

© VNU-HCM Press. This is an open-access article distributed under the terms of the Creative Commons Attribution 4.0 International license.



## ABSTRACT

**Introduction:** Hydrogen fuel cell is a promising renewable energy technology. Proton exchange membranes (PEMs) are an essential component of the fuel cell. Although the top surface nature of PEMs directly relates to the durability and efficiency of PEM fuel cells (PEMFC), there has been very limited attention on the chemical compositions and their distribution at the membrane surface. Thus, this study reports the surface characterization of poly(styrene sulfonic acid) (PSSA)-grafted poly(ethylene-co-tetrafluoroethylene) polymer electrolyte membranes (ETFE-PEMs) for fuel cell applications using S2p X-ray photoelectron spectroscopic (XPS) analysis. **Methods:** The ETFE-PEMs were prepared by radiation-induced grafting and subsequent sulfonation. The surface features of ETFE-PEMs with grafting degrees (GDs) of 55-101% were characterized using the survey-wide and narrow scans of S2p XPS. **Results:** The surface concentration of sulfur slightly decreased with increasing GDs. This interesting result has not been reported in the other graft-type PEMs. The four-component model of narrow scan deconvolution exhibited more reasonable results than the two-component model, in which the sulfonic acid groups ( $\text{SO}_3^-$ ) slightly increased with increasing GDs, not as the case observed by wide scan spectra due to the presence of by-products. **Conclusion:** The PSSA grafts were mainly generated inside the bulk rather than at the surface possibly due to the morphological changes. Moreover, the less presence of  $\text{SO}_3^-$  group on the membrane surface despite the large GD values (GD = 55-101%) suggests the advanced electrolyte properties and interfacial stability for fuel cell applications.

**Key words:** Radiation grafting, surface concentration, polymer electrolyte membranes, X-ray photoelectron spectroscopic

## INTRODUCTION

Polymer electrolyte membrane fuel cell (PEMFCs) have been considered one of the most promising and competitive energy-conversion sectors because of their high efficiency, operation at relatively low temperatures, short start-up process, and transient-response times compared to other fuel cell types<sup>1,2</sup>. The most important part of PEMFCs is polymer electrolyte membrane (PEM), which performs the proton transportation from anode to cathode and separator to  $\text{H}_2$  and  $\text{O}_2$  permeation through the PEM. Nowadays, PEMFCs have been widely used in transportation, stationary, and portable applications<sup>3</sup>. Especially, it has been mainly utilized in commercial electric vehicles such as Nexo 2019 (Hyundai), Mirai 2020 (Toyota), Clarity 2020 (Honda), etc.<sup>4</sup>. However, the main challenge in their development is stability. Critically, the membrane-electrode assemblies (MEAs) in the fuel cell system have been found to degrade after only a few hundred hours at operating temperatures of 60–70 °C<sup>5</sup>. Recently, Schulze et

al.<sup>6</sup> reported the surface decomposition induced the performance loss after 1000 h of fuel cell operation. Therefore, current understanding has suggested that the changes in the PEM surface features can cause poor membrane-electrode interfacial properties. This interfacial property should relate to the MEA delamination and chemical degradation of PEMs<sup>7,8</sup>. Thus, further detailed investigations of surface chemical compositions of PEMs are necessary. The PEMs prepared using irradiation-induced grafting and subsequent sulfonation has been intensively investigated for fuel cell applications over the past 30 years<sup>9–12</sup>. Using this technique, many graft-type PEMs have been prepared successfully such as poly(styrene sulfonic acid) (PSSA)-grafted onto poly(ethylene) (PE-PEM)<sup>8</sup>, poly(tetrafluoroethylene-co-hexafluoropropylene) (FEP-PEM)<sup>9</sup>, poly(tetrafluoroethylene-co-perfluorovinyl ether) (PFA-PEM)<sup>10</sup>, poly(tetrafluoroethylene) (PTFE-PEM)<sup>11,12</sup>, alicyclic polyimides (API-PEM)<sup>13</sup>, and poly(ethylene-co-tetrafluoroethylene) (ETFE-PEM)<sup>14–22</sup>. The surface studies of these graft-type

**Cite this article :** Hao L H, Hieu D T T, Danh T T, Long T H, Phuong H T, Luan L Q, Man T V, Tuyen L A, Ngoc P K, Tap T D. **Surface features of polymer electrolyte membranes for fuel cell applications: An approach using S2p XPS analysis.** *Sci. Tech. Dev. J.*; 24(3):2100-2109.

PEMs have suggested that the specific elemental compositions (i.e., C, F, O, and S) at the surface layers significantly influence their interfacial properties and chemical stability. In other words, it has an impact on the PEMFC performance. Especially, the sulfur concentration is an important indicator of surface feature because it is one of the components of sulfonic acid groups, i.e., the functional conducting groups. These groups relate strongly to the various physical-chemical properties of PEMs, such as ion exchange capacity, water uptake, conductance, swelling, mechanical strength, etc. These properties, in turn, involve the efficiency and durability of PEM fuel cells closely. However, there have been no detailed reports on this component feature.

Moreover, there has been no report on this issue for the ETFE-PEMs, which have been recently recognized as a superior membrane among fully or partially fluorinated graft-type PEMs<sup>14-22</sup>. In detail, the chemical structures of ETFE-PEMs<sup>14,15</sup> and their morphological changes<sup>16-22</sup> have been previously well-studied using other characterizations, except for the graft distribution at the surface layers and within the bulk due to the shortage of meaningful data. Hence, the objective of this study is to report on the surface characterization of ETFE-PEMs using S2p XPS analyses, which is a reasonable representation to evaluate the evolution of functional PSSA grafts with increasing GDs. Based on the results obtained from XPS measurements, the relationship between the surface features and the chemical degradation and electrolyte properties for fuel cell applications is also discussed.

## EXPERIMENTAL

### Materials

The commercial 50- $\mu\text{m}$ -thickness ETFE films were purchased from AGC, Ltd. (Japan), and other chemicals (i.e., styrene, 1,2-dichloroethane, acetone, toluene, and chlorosulfonic acid) were provided from Wako Pure Chemical Industries, Ltd. (Japan). All the chemical substances were then used without further purification. Water was purified using a Millipore Milli-Q UV system producing a resistance of 18.2 M $\Omega$ .cm and total organic carbon content of < 10 ppb.

### ETFE-PEM preparation

The general procedures for preparation and chemical structures of ETFE, grafted ETFE, and ETFE-PEM are depicted in Figure 1. The preparations were comprehensively described in our recent publications<sup>14,15</sup>.

Thus, the present study just shortly outlines it as follows. The ETFE films were irradiated by g-rays emitted from the <sup>60</sup>Co source under argon conditions with an absorbed dose of 15 kGy and a dose rate of 15 kGy/h. The irradiated samples were then immersed in a styrene/toluene mixture with different concentrations at 60 °C for graft polymerization to obtain polystyrene-grafted ETFE (grafted-ETFE) films. The grafted films were then soaked in a 0.2 M chlorosulfonic acid solution in a 1,2-dichloroethane at 50 °C (about 6 hours) for sulfonation. The membrane were finally hydrolysis by pure water at 50 °C for 24 h to obtain ETFE-PEMs<sup>13,14</sup>.

### Characterization

The grafting degree (GD) is determined based on the formula:  $GD (\%) = 100(W_g - W_o)/W_o$ , where  $W_o$  and  $W_g$  are, respectively, the mass of the sample before and after the grafting process. This is the main factor in defining the amount of grafted materials during the propagation. Besides, the sulfonation degree (SD), which is defined as the number of available sulfonic acid groups, is determined by acid-base back titration using an automatic titrator (HIRANUMA COM-555) as the following equation<sup>14,15</sup>:  $SD (\%) = 0.01V_{NaOH} \times 100(100+GD)/(dry\ weight\ of\ membrane \times GD)$ , where  $V_{NaOH}$  is the consumed volume (ml) of the 0.01 M NaOH solution. Other electrolyte properties of ETFE-PEMs, such as water uptake, ion exchange capacity, proton conductivity, and mechanical strength, were described in the previous papers<sup>14,15</sup>.

### XPS measurement

Figure 2 shows the schematically basic principle of XPS measurement. This surface-sensitively quantitative technique gives the empirical formula, chemical and electronic states of the elements existing within a material surface. XPS spectra are obtained by irradiating the sample with the focus X-ray beam. At the same time, the number of electrons and their kinetic energy (KE) escaping from its top layers of 1-10 nm are recorded. Because the incident X-ray energy ( $E_i = h\nu$ ) equals a known quantity and the same calibrated Fermi levels as shown in Figure 2, the electron binding energy (BE) of the ejected electrons can be directly determined through the work function of the spectrometer ( $\phi_{spec}$ ) by using the following equation (1):

$$BE = E_i - KE - \phi_{spec} \quad (1)$$

The surface chemical compositions of all samples were measured using a Thermo Fisher K-Alpha spectrometer equipped with a hemispherical analyzer. A

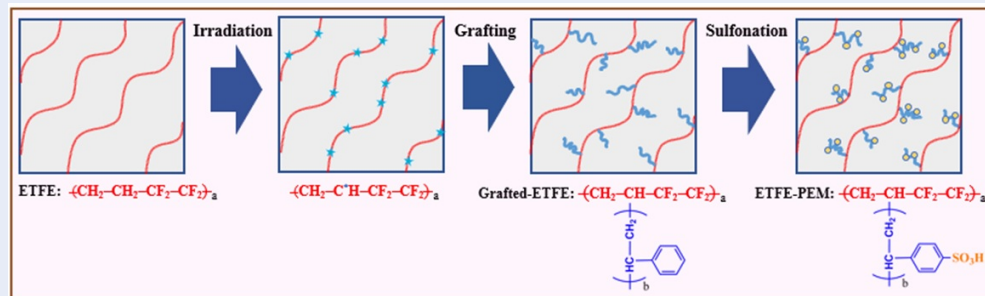


**Figure 1: Preparation procedure and chemical structures of ETFE, grafted ETFE, and ETFE-PEMs .** The membranes were prepared using pre-irradiated grafting of styrene onto the ETFE substrate and subsequent sulfonation.

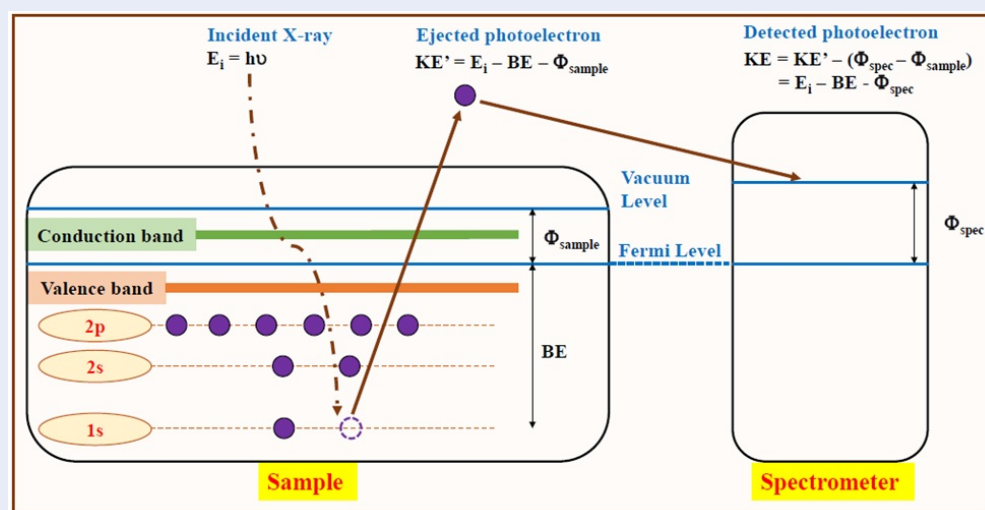


**Figure 2: Schematic of the principles of XPS .** A typical XPS spectrum is a plot of the number of detected electrons versus their corresponding BE. Each element near the surface region produces a specific set of peaks at characteristic BEs.

monochromatic X-ray Al K $\alpha$  source ( $h\nu = 1486.6 \text{ eV}$ ) with a voltage of 12 kV and an emission current of 3 mA was employed. The beam spot size is 400  $\mu\text{m}$  for all spectra, while a compensating electron flood gun was used for surface charge neutralization to minimize the charging effect under a maintained pressure of ultrahigh vacuum ( $10^{-7} \text{ mbar}$ ). An energy scale of the concentric hemispherical analyzer system was tested with quality control procedures and adjusted in accordance with Au4f (84.0 eV), Ag3d (368.2 eV), and Cu2p (932.6 eV) lines of standards before measurements to ensure reproducible results within acceptable limits. Namely, the repeated statistical quality of the acquired spectral data (30 scans) can be used for the transfer of meaningful data without any further statistical analysis. These intensity data of ETFE-

PEMs are then evaluated by other repeated spectra (i.e., divide this by the initial spectrum as a function of kinetic energy) to confirm that no significant change has occurred to the sample or spectrometer during acquisition<sup>23</sup>. In S2p levels, precision may vary by only a few tenths of percentages due to its moderate photoelectron cross-sections<sup>24</sup> for the 1486.6 eV Al K $\alpha$  lines. Thus, the accuracy of the relative sensitivity factors is as good as 1.881, given a minor error ( $\sim 2\text{-}10\%$ ) compared to other surface analyses such as atomic force microscope (AFM), low energy electron diffraction (LEED), electron energy loss spectroscopy (ELS), etc.<sup>25</sup> XPS spectra were recorded with an analyzer pass energy of 100.0 eV (step size = 0.5 eV) for the survey scan and 20.0 eV (step size = 0.05 eV) for the narrow scans. Atomic concentrations were then

manipulated and quantified using the CasaXPS (version 2.2.107). The narrow scan analyses are conducted by using PeakFit (version 4.12) data processing software. The deconvolution of narrow scan spectra was performed with the considerable assignment of peak component, is ensured by the good quality of the raw data (i.e., the energy resolution and signal to noise), the high-resolution XPS of organic polymer database<sup>26</sup>, and the relevant graft-type PEM reports<sup>8-12,27,28</sup>. The restricted full width at half maximum (FWHM) values was also conducted to obtain the meaningful component percentages.

## RESULT

Figure 3 illustrates the survey-wide scan spectra of ETFE-PEMs in the GD range of 55-101%. Characteristic functional grafted chains, i.e., the PSSA groups, can be elucidated based on S2p representative due to the presence of the sulfonic acid group ( $\text{SO}_3^-$ ) generated by the sulfonation process<sup>26-28</sup>. Namely, peaks at ca. 169.1 eV for GDs at 55 and 77% and 169.6 eV for a GD of 101% are ascribed to the S2p feature of sulfonic acid groups<sup>8-12</sup>. Therefore, increasing GD results in a change in those peak intensities and areas. The calculated atomic concentrations are represented in Table 1. The results show that the sulfur concentrations slightly decrease from 6.1 to 4.9%, with GDs ranging from 55 to 101%, corresponding to SDs of 87-83%.

Figure 4a represents the narrow scan of S2p spectra of ETFE-PEMs having various GDs. A predominant peak at the lower BE region (168.2-168.6 eV) is observed together with another weaker one locates at, the higher BE (169.4-169.8 eV). Because the S2p core level consists of two well-defined total angular momentum quantum numbers ( $j$ ) of 1/2 and 3/2, this doublet of the line shape reveals the characteristic S2p<sub>3/2</sub>-S2p<sub>1/2</sub> spin-orbit splitting. Namely, the degeneracy or the area ratio between the lower and higher  $j$  values is given by 2:1, corresponding to, respectively, 4 and 2 electrons in the 2p<sub>3/2</sub> and 2p<sub>1/2</sub> levels<sup>29</sup>. To further investigate the changes taking place in the surface compositions, the S2p core level spectra are deconvoluted via two models. The first model is based on the assumption that only the main product of sulfonic acid groups ( $\text{SO}_3^-$ ) exists in the membranes. A similar assumption was also reported in sulfonated silica/Nafion<sup>30</sup> and sulfonated PEEK membranes<sup>31</sup>. In this case, the S2p spectra are deconvoluted into two components (two-component model) with BEs of 168.4 and 169.6 eV (Figure 4b). These peaks are reasonably assigned to two characteristic spin-orbit components of S2p, i.e., 2p<sub>3/2</sub> and

2p<sub>1/2</sub> of  $\text{SO}_3^-$ . The second model is based on the assumption that the membranes contain the main product of  $\text{SO}_3^-$  plus other by-products such as S-C, S=C, S=O ( $\text{SO}_2^-$ ), S-Cl, etc. In this case, the S2p spectra are deconvoluted into four components (four-component model) with BEs of 167.3, 168.5, 168.9, and 169.7 eV. The two major peaks at 168.5 and 169.6 eV are assigned to the higher oxidation state of  $\text{SO}_3^-$ , as the case of two-component model. Meanwhile, the remaining minor peaks at 167.3 and 168.9 eV are attributed to the 2p<sub>3/2</sub> and 2p<sub>1/2</sub> of the lower oxidation state of by-products due to their electronegativity. The undesired reactions may form these by-products during the sulfonation process<sup>9,11,12,32</sup>. All the chemical characteristics for a pair of spin-orbit splitting are separated by a DBE of nearly 1.18 eV and given concentration ratios of nearly 2.0, which is a complete agreement with those in the literature<sup>26,29,30</sup>.

Figure 5 shows all the deconvoluted results of ETFE-PEMs with GDs of 55-101%. The corresponding parameters of each component of deconvolution, such as BE, FWHM, and concentration percentage, are represented in Table 2. For the two-component model (Figures 5a and 5b), it can be seen that the BEs of 2p<sub>3/2</sub> and 2p<sub>1/2</sub> peaks show almost no shifts (168.7-168.3 and 169.9-169.5 eV, respectively). The corresponding FWHM values are also constrained (1.07-1.14 and 1.18-1.21 eV) over the entire GD range. Meantime, the concentration percentages of those states are varied unclear, e.g., from 67.8 to 72.8 then 68.3% (for 2p<sub>3/2</sub>) and from 32.2 to 27.2 and 31.7% (for 2p<sub>1/2</sub>). On the other hand, for the four-component model, the spectra feature of  $\text{SO}_3^-$  and S-X (S-C, S=C, S=O ( $\text{SO}_2^-$ ), S-Cl, etc.) in Figure 5c-f exhibit the stabilized BEs within 168.3-170.0 and 167.3-169.4 eV, and the constrained FWHM values of 1.00-1.21 and 0.9-1.33 eV, respectively. Interestingly, the peak positions and peak widths in both models are the same despite the presence of additional S-X species. However, the two-component model results in suspectable percentages, i.e., the unclear trends of S2p<sub>3/2</sub> with GDs of 55-77% and 77-101%. In contrast, the four-component model shows the clear trend of S2p<sub>3/2</sub> and S2p<sub>1/2</sub> components with increasing GD.

## DISCUSSION

The surface sulfur concentration representatives of ETFE-PEMs show only a gradual decrease as compared with the high increase of GD from 55 to 101%, corresponding to SDs from 87 to 83% (Table 1). The result suggests less PSSA graft chains at the surface layers of membranes rather than in their bulk. This

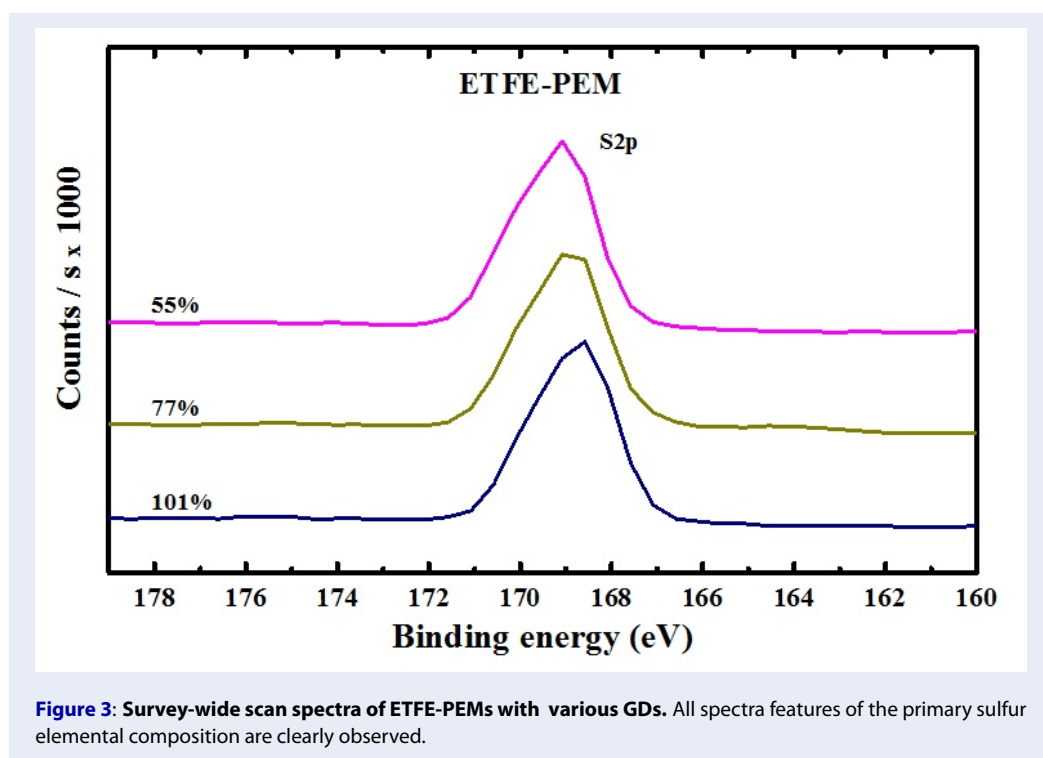


**Table 1: The values of BEs and sulfur atomic concentration of the ETFE-PEMs with various GDs and SDs**

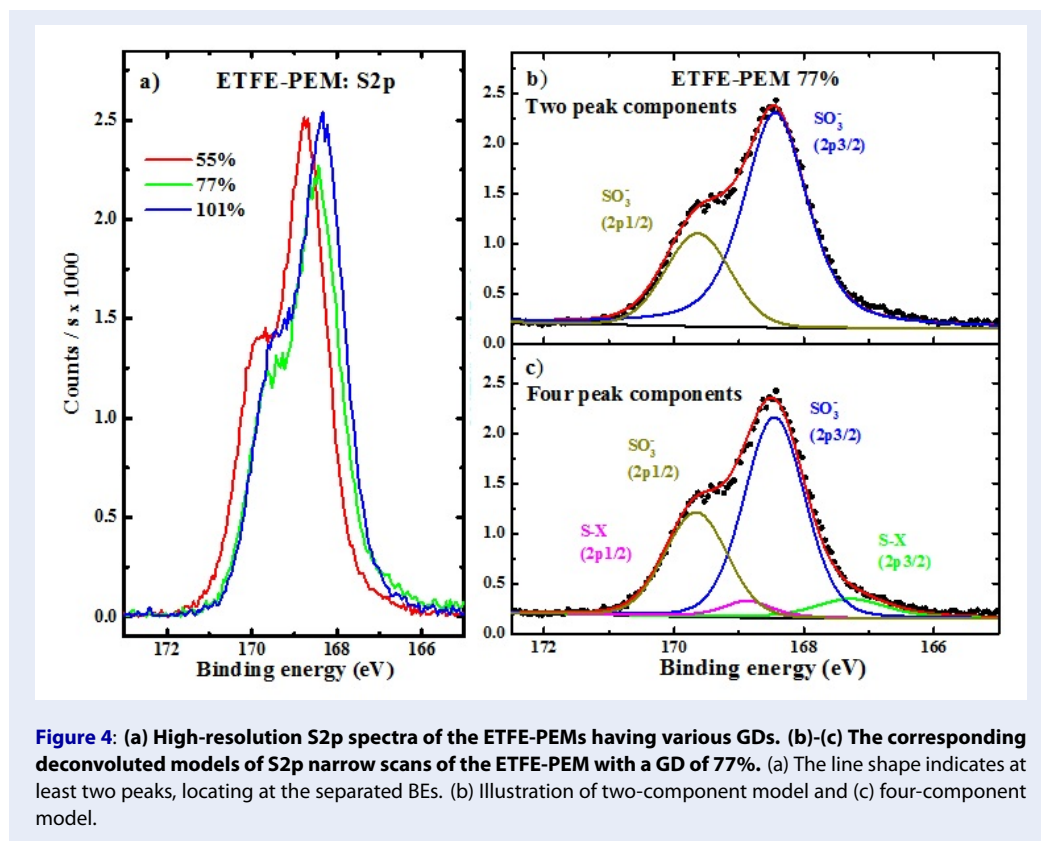
GD (%)	55	77	101
SD (%)	87	85	83
BE (eV)	169.1	169.1	169.6
Sulfur concentration (%)	6.1	5.7	4.9

observation is quite interesting because it is a conventional acceptance that the higher GD, the higher amount of PSSA grafts at the surface is obtained. The result is totally different from that of the API-PEMs, in which the surface accumulation was accelerated with increasing the PSSA grafts (GD = 0-70%)<sup>13</sup>. Moreover, it has also been reported in other graft-type PEMs<sup>12,33</sup> that the sulfur concentration increased with increasing GD (GD < 50%). For instance, the sulfur concentration increased from 4.5 to 6.5% for PTFE-PEMs with GDs of 8-36%<sup>12</sup> and from 3.9 to 5.8 for LDPE-PEMs with GDs of 11-48%<sup>33</sup>. One possible explanation for the gradual decrease in the surface sulfur concentration of ETFE-PEMs in the GD range of 59-79% is due to the phase transition from oriented crystallite to crystallite network structures, as revealed in our previous reports<sup>16,17</sup>. This phase transition may allow more PSSA grafts to generate in bulk rather than at the surface. Another possible reason is that the partial PSSA grafts may be diffused

into the bulk due to the swelling effects at high GDs. Generally, it is conventionally believed that most of the grafting polymerizations occur in the fully or partially fluorinated substrates according to the grafting front mechanism<sup>34</sup>. The initial grafting chains take place at the surface firstly. These grafted layers then swell in the grafting medium as the diluent, which acts as a solvent for the grafted chains (PSSA) and further diffuse into the membrane bulk. Longer grafting time and more monomer concentration result in the diffusion of the monomer through swollen grafted zones till the “grafting front” toward the middle of the membrane at the higher GD. Although the ability of generated radicals to capture styrene molecules highly depends on the number of active centers and monomer concentration, the subsequent propagation and termination steps are highly induced by the grafting medium. In other words, the higher swelling of the grafted zone, the higher monomer availability to the grafting sites<sup>35</sup>. Accordingly, in ETFE-based

**Table 2: The deconvoluted results (BEs, FWHM, and percentage) of S2p spectra of ETFE-PEMs with GD = 55- 101%. These results are obtained by using the two-component model and four-component model**

Model	GD (%)	BE (eV)			FWHM (eV)			Percentage (%)		
		SO <sub>3</sub> <sup>-</sup> (2p3/2)	SO <sub>3</sub> <sup>-</sup> (2p1/2)	S-X (2p3/2)	SO <sub>3</sub> <sup>-</sup> (2p1/2)	SO <sub>3</sub> <sup>-</sup> (2p3/2)	S-X (2p1/2)	SO <sub>3</sub> <sup>-</sup> (2p1/2)	SO <sub>3</sub> <sup>-</sup> (2p3/2)	S-X (2p1/2)
Two-component model	55	168.7	169.9	-	1.07	1.21	-	67.8	32.2	-
	77	168.4	169.6	-	1.16	1.18	-	72.8	27.2	-
	101	168.3	169.5	-	1.14	1.21	-	68.3	31.7	-
Four-component model	55	168.7	170.0	168.0	1.03	1.00	1.21	57.4	29.6	8.3
	77	168.5	169.7	167.3	1.10	1.13	1.33	57.6	29.9	7.7
	101	168.3	169.5	167.3	1.13	1.21	1.29	59.8	31.5	6.0



grafted PEM, toluene is well-known as a good solvent for polystyrene and swell the ETFE film<sup>36,37</sup>, and even good at solvating grafted PS in ETFE-g-PS<sup>38</sup>. Therefore, this behavior should be related to the low accumulation of PSSA grafts at the membrane surface. Moreover, the by-products may also partially affect the above trend of surface sulfur concentration. Noted that the less accumulation of PSSA grafts on the membrane surface should be considered a significant advantageous property of ETFE-PEMs for fuel cell application because it reduces the membrane brittleness and/or less chemical degradation<sup>8,12</sup>.

As presented in Table 2, the four-component model reflects well the surface features, and thus, its results are used to discuss further. Over the entire GD range, the percentages of the sole product of  $\text{SO}_3^-$  always dominate on the membrane surfaces (87.0-91.3%), while that of the by-product groups are steadily depleted (13.0-8.7%). Thus, the sulfonic acid groups play a key role on the top layers, affecting the interfacial properties<sup>12,29,39</sup>. Particularly, although the high increase of GD from 55 to 101% provides a large content of the incorporated PSSA grafts, there is only a slow accumulation of sulfonic acid groups ( $\%\text{SO}_3^- = 87.0\text{-}91.3\%$ ) on the top layers of membranes. Be-

cause the PSSA graft chains could be generated either at the surface or bulk of the ETFE-PEMs but not follow the front mechanism<sup>38</sup>, this observation suggests more PSSA grafts inside the bulk. The increase of  $\text{SO}_3^-$  components using a four-component model (Table 2) is by the corresponding electrochemical properties such as ion exchange capacity and proton conductivity of the same ETFE-PEMs with increasing GD as reported previously<sup>15</sup>. In such a case, the high IEC of ETFE-PEMs clearly assists the presence of more  $\text{SO}_3^-$  groups in the bulk rather than on the surface, leading to the competitive proton conductivity to those of the commercial Nafion-212<sup>14,15</sup>. Moreover, as mentioned above, this significant surface signature of ETFE-PEMs should show less brittleness and/or less chemical degradation<sup>8,12</sup>, displaying an advantageous property for fuel cell applications.

## CONCLUSION

The surface sulfur concentration of the ETFE-PEMs prepared by pre-irradiated grafting within the GD range of 55-101% was investigated by using S2p XPS analysis. The obtained results indicate that the membrane surfaces were less accumulation of PSSA grafts. Moreover, among all possible sulfonation products,

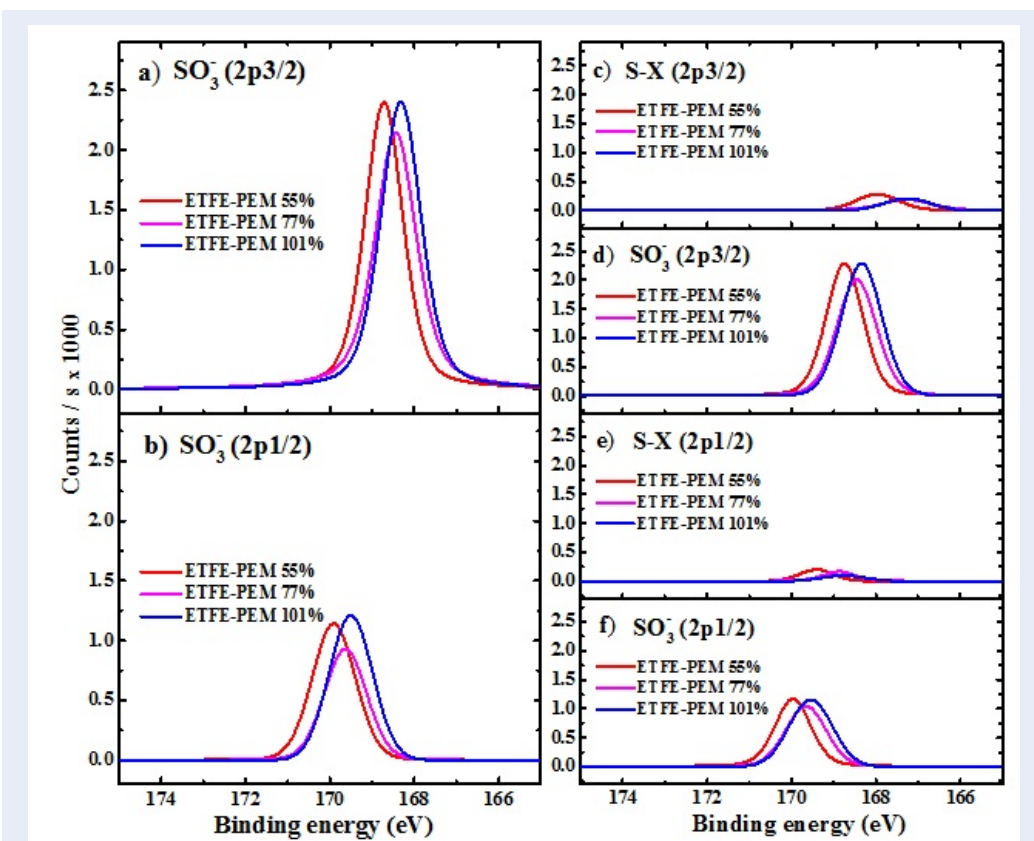


**Figure 5:** The characteristic spin-orbit components of S2p of the ETFE-PEMs with various GDs. (a) and (b) Deconvoluted peaks using the two-component model. (c)-(f) Deconvoluted peaks using the four-component model.

the sulfur species originated from sulfonic acid groups ( $\text{SO}_3^-$ ) are predominance. The less sulfur concentration at the surface layers and the only steady increase of  $\text{SO}_3^-$  with a high increase of GD indicate that the PSSA grafts were mainly generated inside the bulk rather than on the membrane surface due to the morphological changes. Therefore, all the above observations should provide a further understanding of the important role of  $\text{SO}_3^-$  groups in the interfacial properties, and thus, the stability. It shows the significant advantages of graft-type ETFE-PEMs in term of surface properties for the PEMFC applications.

## LIST OF ABBREVIATIONS

ETFE: Poly(Ethylene-co-TetraFluoroEthylene)

PEMFC: Polymer Electrolyte Membranes Fuel Cell

IEC: Ion Exchange Capacity

XPS: X-ray Photoelectron Spectroscopy

GD: Grafting Degree

PS: Poly Styrene

PSSA: Poly Styrene Sulfonic Acid

## COMPETING INTERESTS

There are no conflicts of interest to declare.

## ACKNOWLEDGMENTS

This research is funded by Vingroup Big Data Institute (VINBIGDATA), Vingroup and supported by Vingroup Innovation Foundation (VINIF) under project code VINIF.2020.DA08.

## AUTHORS CONTRIBUTION

**Tran Duy Tap:** Conceptualization, Project administration, Funding acquisition, Supervision, Resources, Investigation, Methodology, Data curation, Formal analysis, Supervision, Validation, Visualization, Writing - original draft, Writing - review & editing. **Lam Hoang Hao:** Investigation, Methodology, Data curation, Formal analysis, Validation, Visualization, Writing - original draft, Writing - review & editing. **Dinh Tran Trong Hieu:** Visualization, Validation, Writing - review & editing. **Tran Thanh Danh and Tran Van Man:** Visualization, Validation. **Tran Hoang Long:**



Visualization, Investigation. **Huynh Truc Phuong and Le Quang Luan:** Visualization. **Luu Anh Tuyen and Pham Kim Ngoc:** Visualization, Validation, Data curation.

## REFERENCES

- Borup R, Meyers J, Pivovar B, Kim YS, Mukundan R, Garland N, Myers D, Wilson M, Garzon F, Wood D, Zelenay P, Zelenay P, More K, Stroh K, Zawodzinski T, Boncella J, McGrath JE, Inaba M, Miyatake K, Hori M, Ota K, Ogumi Z, Miyata S, Nishikata A, Siroma Z, Uchimoto Y, Yasuda K, Kimjima K, Iwashita N. Scientific aspects of polymer electrolyte fuel cell durability and degradation. *Chem Rev.* 2007;107(10):3904-3951;PMID: 17850115. Available from: <https://doi.org/10.1021/cr050182l>.
- Wang S, Jiang SP. Prospects of fuel cell technologies. *Natl Sci Rev.* 2017;4(2):163-166; Available from: <https://doi.org/10.1093/nsr/nww099>.
- Sharaf OZ, Orhan MF. An overview of fuel cell technology: Fundamentals and applications. *Renew Sustain Energy Rev.* 2014;32:810-853; Available from: <https://doi.org/10.1016/j.rser.2014.01.012>.
- Lü X, Qu Y, Wang Y, Qin C, Liu G. A comprehensive review on hybrid power system for PEMFC-HEV: Issues and strategies. *Energy Convers Manag.* 2018;171:1273-1291; Available from: <https://doi.org/10.1016/j.enconman.2018.06.065>.
- Gode P, Ihonen J, Strandroth A, Ericson H, Lindbergh G, Paronen M, Sundholm F, Sundholm G, Walsby N. Membrane durability in a PEM fuel cell studied using PVDF based radiation grafted membranes. *Fuel Cells.* 2003;3(1-2):21-27; Available from: <https://doi.org/10.1002/face.200320239>.
- Schulze M, Wagner N, Kaz T, Friedrich KA. Combined electrochemical and surface analysis investigation of degradation processes in polymer electrolyte membrane fuel cells. *Electrochim Acta.* 2007;52(6):2328-2336; Available from: <https://doi.org/10.1016/j.electacta.2006.05.063>.
- Horsfall JA, Lovell KV. Fuel cell performance of radiation grafted sulphonic acid membranes. *Fuel Cells.* 2001;1(3-4):186-191; Available from: [https://doi.org/10.1002/1615-6854\(200112\)1:3/4<186::AID-FUCE186>3.0.CO;2-A](https://doi.org/10.1002/1615-6854(200112)1:3/4<186::AID-FUCE186>3.0.CO;2-A).
- Sherazi TA, Guiver MD, Kingston D, Ahmad S, Kashmiri MA, Xue X. Radiation-grafted membranes based on polyethylene for direct methanol fuel cells. *J Power Sources.* 2010;195(1):21-29; Available from: <https://doi.org/10.1016/j.jpowsour.2009.07.021>.
- Nasef MM, Saidi H, Yarmo MA. Surface investigations of radiation grafted FEP-g-polystyrene sulfonic acid membranes using XPS. *J New Mater Electrochem Syst.* 2000;3(4):309-318; Available from: [https://www.researchgate.net/profile/Mohamed-Nasef-3/publication/268241789\\_Surface\\_investigations\\_of\\_radiation\\_grafted\\_FEP-g-polystyrene\\_sulfonic\\_acid\\_membranes\\_using\\_XPS/links/54cb33860cf22f98631e4139/Surface-investigations-of-radiation-grafted-FEP-g-polystyrene-sulfonic-acid-membranes-using-XPS.pdf](https://www.researchgate.net/profile/Mohamed-Nasef-3/publication/268241789_Surface_investigations_of_radiation_grafted_FEP-g-polystyrene_sulfonic_acid_membranes_using_XPS/links/54cb33860cf22f98631e4139/Surface-investigations-of-radiation-grafted-FEP-g-polystyrene-sulfonic-acid-membranes-using-XPS.pdf).
- Nasef MM, Saidi H, Ambar M. Cation exchange membranes by radiation-induced graft copolymerization of styrene onto PFA copolymer films. IV. Morphological investigations using X-ray photoelectron spectroscopy. *J Appl Polym Sci.* 2000;77(11):2455-2463; Available from: [https://doi.org/10.1002/1097-4628\(20000912\)77:11<32455::AID-APP14%3E3.0.CO;2-5](https://doi.org/10.1002/1097-4628(20000912)77:11<32455::AID-APP14%3E3.0.CO;2-5).
- Nasef MM, Saidi H, Nor HM, Yarmo MA. XPS studies of radiation grafted PTFE-g-polystyrene sulfonic acid membranes. *J Appl Polym Sci.* 2000;76(3):336-349; Available from: [https://doi.org/10.1002/\(SICI\)1097-4628\(20000418\)76:3<336::AID-APP9>3.0.CO;2-E](https://doi.org/10.1002/(SICI)1097-4628(20000418)76:3<336::AID-APP9>3.0.CO;2-E).
- Nasef MM, Saidi H. Surface studies of radiation grafted sulfonic acid membranes: XPS and SEM analysis. *Appl Surf Sci.* 2006;252(8):3073-3084; Available from: <https://doi.org/10.1016/j.apsusc.2005.05.013>.
- Park J, Enomoto K, Yamashita T, Takagi Y, Todaka K, Maekawa Y. Polymerization mechanism for radiation-induced grafting of styrene into alicyclic polyimide films for preparation of polymer electrolyte membranes. *J Membr Sci.* 2013;438:1-7; Available from: <https://doi.org/10.1016/j.memsci.2013.03.007>.
- Tap TD, Nguyen LL, Hien NQ, Thang PB, Sawada SI, Hasegawa S, Maekawa Y. Humidity and temperature effects on mechanical properties and conductivity of graft-type polymer electrolyte membrane. *Radiat Phys Chem.* 2018;151:186-191; Available from: <https://doi.org/10.1016/j.radphyschem.2018.06.033>.
- Tap TD, Sawada SI, Hasegawa S, Katsumura Y, Maekawa Y. Poly (ethylene-co-tetrafluoroethylene)(ETFE)-based graft-type polymer electrolyte membranes with different ion exchange capacities: Relative humidity dependence for fuel cell applications. *J Membr Sci.* 2013;447:19-25; Available from: <https://doi.org/10.1016/j.memsci.2013.07.041>.
- Tap TD, Sawada S, Hasegawa S, Yoshimura K, Oba Y, Ohnuma M, Katsumura Y, Maekawa Y. Hierarchical structure—property relationships in graft-type fluorinated polymer electrolyte membranes using small- and ultrasmall-angle X-ray scattering analysis. *Macromolecules.* 2014;47(7):2373-2383; Available from: <https://doi.org/10.1021/ma500111x>.
- Tap TD, Nguyen LL, Zhao Y, Hasegawa S, Sawada SI, Hung NQ, Maekawa Y. SAXS investigation on morphological change in lamellar structures during propagation steps of graft-type polymer electrolyte membranes for fuel cell applications. *Macromol Chem Phys.* 2020;221(3):1900325; Available from: <https://doi.org/10.1002/macp.201900325>.
- Tap TD, Nguyen LL, Hasegawa S, Sawada SI, Luan LQ, Maekawa Y. Internal and interfacial structure analysis of graft-type fluorinated polymer electrolyte membranes by small-angle X-ray scattering in the high-q range. *J Appl Polym Sci.* 2020;137(35):49029; Available from: <https://doi.org/10.1002/app.49029>.
- Nguyen LL, et al. Ứng dụng phương pháp tán xạ tia X góc nhỏ đánh giá ảnh hưởng thẳng giăng mật độ điện tử đến các cấu trúc vi mô của màng dẫn proton trong pin nhiên liệu. *VJST B* [Internet]. 2021;62(1):54-59; Available from: [https://b.vjst.vn/index.php/ban\\_b/article/view/941](https://b.vjst.vn/index.php/ban_b/article/view/941).
- Tap TD. Nghiên cứu cấu trúc của màng điện cực polymer sử dụng cho pin nhiên liệu bằng phương pháp tán xạ tia X góc nhỏ và siêu nhỏ. *VJST B* [Internet]. 2018;60(8):8-11; Available from: [https://b.vjst.vn/index.php/ban\\_b/article/view/624](https://b.vjst.vn/index.php/ban_b/article/view/624).
- Tap TD, et al. Nghiên cứu cấu trúc màng điện cực polymer sử dụng tán xạ tia X góc hẹp và phổ bức xạ hủy positron. *STDJNS.* 2017;20:197-205; Available from: [http://www.google.com/url?sa=t&rct=j&q=&esrc=s&source=web&cd=&cad=rja&uact=8&ved=2ahUKewiQ6878mq\\_wAhWQ8HMBHWcCAzEQFjAAegQIAXAD&url=http%3A%2Fstdjns.scienceandtechnology.com.vn%2Findex.php%2Fstdjns%2Fdownload%2F30%2F60%2F&usq=AOvVaw3Dx9ay5dhX4Y3xKGpkvELJ](http://www.google.com/url?sa=t&rct=j&q=&esrc=s&source=web&cd=&cad=rja&uact=8&ved=2ahUKewiQ6878mq_wAhWQ8HMBHWcCAzEQFjAAegQIAXAD&url=http%3A%2Fstdjns.scienceandtechnology.com.vn%2Findex.php%2Fstdjns%2Fdownload%2F30%2F60%2F&usq=AOvVaw3Dx9ay5dhX4Y3xKGpkvELJ).
- Tap TD, et al. Study of lamellar structures of graft-type fluorinated proton exchange membranes by small-angle X-ray scattering: preparation procedures and grafting degree dependence for fuel application. *STDJNS.* 2015;8:153-161; Available from: <https://doi.org/10.32508/stdj.v18i3.831>.
- Shard AG, Spencer SJ. Intensity calibration for monochromated Al K $\alpha$  XPS instruments using polyethylene. *Surf Interface Anal.* 2019;51(6):618-626; Available from: <https://doi.org/10.1002/sia.6627>.
- Scofield JH. Hartree-Slater subshell photoionization cross-sections at 1254 and 1487 eV. *J Electron Spectrosc Relat Phenom.* 1976;8(2):129-137; Available from: [https://doi.org/10.1016/0368-2048\(76\)80015-1](https://doi.org/10.1016/0368-2048(76)80015-1).
- Rivière JC. Surface analysis: current capabilities. *Mater Sci Technol.* 1993;9(5):365-377; Available from: <https://doi.org/10.1179/mst.1993.9.5.365>.

26. Beamson G, Briggs D. High Resolution XPS of Organic Polymers: The Scienta ESCA300 Database. Wiley: Chichester, 1992:31-32;.
27. Çelik G, Barsbay M, Güven O. Towards new proton exchange membrane materials with enhanced performance via RAFT polymerization. *Polym Chem*. 2016;346(1):701-714; Available from: <https://doi.org/10.1039/C5PY01527H>.
28. Everett ML, Hoflund GB. Erosion study of poly(ethylene tetrafluoroethylene) (Tefzel) by hyperthermal atomic oxygen. *Macromolecules*. 2004;37(16):6013-6018; Available from: <https://doi.org/10.1021/ma049515r>.
29. Briggs D. XPS: Basic Principles, Spectral Features and Qualitative Analysis, pp. 31-56, in: Briggs D, Grant JT. *Surface Analysis by Auger and X-ray Photoelectron Spectroscopy*. IM Publications. Chichester; 2003. 900 pp;.
30. Yen CY, Lee CH, Lin YF, Lin HL, Hsiao YH, Liao SH, Chuang CY, Ma CCM. Sol-gel derived sulfonated-silica/Nafion® composite membrane for direct methanol fuel cell. *J Power Sources*. 2007;173(1):36-44; Available from: <https://doi.org/10.1016/j.jpowsour.2007.08.017>.
31. Zhao Y, Wong HM, Wang W, Li P, Xu Z, Chong EY, Chu PK. Cytocompatibility, osseointegration, and bioactivity of three-dimensional porous and nanostructured network on polyetheretherketone. *Biomaterials*. 2013;34(37):9264-9277; PMID: 24041423. Available from: <https://doi.org/10.1016/j.biomaterials.2013.08.071>.
32. Yasuda K, Uchimoto Y, Ogumi Z, Takehara ZI. Preparation of Thin Perfluorosulfonate Cation-Exchanger Films by Plasma Polymerization. *J Electrochem Soc*. 1994;141(9):2350; Available from: <https://doi.org/10.1149/1.2055124>.
33. Lukáš J, Tyáčková V. Characterization of ion exchange membrane surfaces by means of X-ray photoelectron spectroscopy and SEM. *J Membr Sci*. 1991;58(1):49-57; Available from: [https://doi.org/10.1016/S0376-7388\(00\)80636-5](https://doi.org/10.1016/S0376-7388(00)80636-5).
34. Gupta B, Büchi FN, Scherer GG. Cation exchange membranes by pre-irradiation grafting of styrene into FEP films. I. Influence of synthesis conditions. *J Polym Sci, Part A: Polym Chem*. 1994;32(10):1931-1938; Available from: <https://doi.org/10.1002/pola.1994.080321016>.
35. Nasef MM. Effect of solvents on radiation-induced grafting of styrene onto fluorinated polymer films. *Polym Int*. 2001;50(3):338-346; Available from: <https://doi.org/10.1002/pi.634>.
36. Kimura Y, Asano M, Chen J, Maekawa Y, Katakai R, Yoshida M. Influence of grafting solvents on the properties of polymer electrolyte membranes prepared by  $\gamma$ -ray preirradiation method. *Radiat Phys Chem*. 2008;77(7):864-870; Available from: <https://doi.org/10.1016/j.radphyschem.2007.12.012>.
37. Geraldes AN, Zen HA, Ribeiro R, Parra DF, Lugão AB. Solvent effect on post-irradiation grafting of styrene onto poly(ethylene-alt-tetrafluoroethylene) (ETFE) films. *Radiat Phys Chem*. 2013;84:205-209; Available from: <https://doi.org/10.1016/j.radphyschem.2012.06.016>.
38. Ko BS, Yoshimura K, Hiroki A, Maekawa Y. Mechanistic study on radiation-induced grafting into fluorinated polymer solid films using a swelling-induced detachment of grafted polymers. *J Polym Sci*. 2021;59:108-116; Available from: <https://doi.org/10.1002/pol.20200727>.
39. Homberg S, Näsman JH, Sundholm F. Synthesis and properties of sulfonated and crosslinked poly [(vinylidene fluoride)-graft-styrene] membranes. *Polym Adv Technol*. 1998;9(2):121-127; Available from: [https://doi.org/10.1002/\(SICI\)1099-1581\(199802\)9:2<121::AID-PAT724>3.0.CO;2-M](https://doi.org/10.1002/(SICI)1099-1581(199802)9:2<121::AID-PAT724>3.0.CO;2-M).